COMPUTATIONAL METHODS IN APPLIED MATHEMATICS, Vol. 9 (2009), No. 3, pp. 238–252


# A MACRO-KINETIC HYBRID MODEL FOR TRAFFIC FLOW ON ROAD NETWORKS

M. HERTY[1] AND S. MOUTARI[2]

**Abstract** — We have developed a new hybrid model for an heterogeneous traffic flow, based on a coupling of the Lighthill — Whitham [23] and Richards [27] (LWR) macroscopic model and the kinetic model introduced in [21]. On the highways of a road network, we consider the macroscopic description of the traffic flow and switch to the kinetic model to compute the mass flux through a junction. This new model reproduces the capacity drop phenomenon at a merge junction, for instance, without imposing any priority rule. We present some numerical simulations in which we compare the results of the hybrid model with those given by the fully macroscopic model. Furthermore, we illustrate the consequences of the velocity distribution on the flow through a merging junction.

**2000 Mathematics Subject Classification:** 35L, 35L65.

**Keywords:** traffic flow, macroscopic model, kinetic model, hybrid model.

## 1. Introduction

The vehicular traffic has been the subject of active research for almost sixty years and various theories have been proposed to model the traffic flow on road networks. Some of them are based on macroscopic models [4, 6, 8, 13, 15–18, 22, 28], others on microscopic models [1, 3, 26], and some are based on Boltzmann or Fokker — Planck type equations [11, 12, 19–21]. However, macroscopic models are known to be somewhat coarse to describe certain situations such as intersections whereas the implementation of microscopic models on large road networks is too complex to handle. Recently, hybrid approaches combining microscopic and macroscopic models [9, 24, 25, ...] have been investigated. Nevertheless, as promising as this approach, it is not as obvious to implement. Indeed, in addition to the compatibility issue between the models to be coupled, the implementation of the interfaces could be a tedious task in practice.

In this paper, we develop a simple hybrid model for road networks based on the coupling of the Lighthill — Whitham and Richards (LWR) macroscopic model [23, 27] and the kinetic type model introduced in [21]. To describe the traffic dynamics on a road network, we proceed as follows: on a highway, we consider the LWR model (which can be derived from the kinetic model in [21]), while at an intersection, in order to describe the traffic dynamics in more detail, we take into account the velocity distribution by considering the kinetic type

[1] *RWTH Aachen University, Mathematik*, Templergraben 55, D-52065 Aachen, Germany. E-mail: herty@mathc.rwth-aachen.de

[2] *CenSSOR David Bates Building, Queen's University Belfast*, University Road, Belfast BT7 1NN, United Kingdom. E-mail: s.moutari@qub.ac.uk

model to compute the mass flux through the junction. This mass flux value is then used to solve the Riemann problem within the macroscopic boundary data. Furthermore, the derivation of the LWR macroscopic model from the kinetic model is immediate (see [21]): Thereby we get rid of the interface problem often encountered when developing a hybrid model.

The remaining part of this paper is as follows. In Section 2, we present the kinetic model introduced in [21], from which we derive the LWR macroscopic model. In Section 3 we introduce a new hybrid model which includes the velocity distribution in traffic flow, whose consequences are illustrated through some numerical simulations in Section 4.

## 2. The models

This section is devoted to the presentation of the models to be coupled in the next section in order to develop our hybrid model. First we present the kinetic model introduced in [21] from which we derive the LWR macroscopic model.

We are concerned with the Boltzmann type model for high density traffic with a braking/acceleration force, introduced in [21]. This model consists of the following equation:

$$\partial_t f + v\partial_x f = C(f), \tag{2.1}$$

where $x, t, v$ denote the position on the road, the time, and the speed, respectively; $f = f(x,t,v)$, $\rho = \rho(x,t)$ and $u = u(x,t)$ denote the kinetic density, the macroscopic density, and the macroscopic velocity, respectively, whereas $C(f)$ is a function of the gain and loss terms due to the braking and acceleration. It can be modelled in serveral ways and we refer the reader to [21] for a detailed discussion. Its main property is

$$\int_0^{v_{\max}} C(f)\, dv = 0.$$

This is used in the following derivation. Multiplying the kinetic equation (2.1) by $\phi(v)$ and integrating it with respect to $v$, we obtain

$$\partial_t \int_0^{v_{\max}} \phi(v) f\, dv + \partial_x \int_0^{v_{\max}} v\phi(v) f\, dv = \int_0^{v_{\max}} \phi(v) C(f), \tag{2.2}$$

For $\phi(v) = 1$ we obtain

$$\partial_t \rho + \partial_x(\rho u) = 0 \tag{2.3}$$

if we set

$$\rho = \int_0^{v_{\max}} f\, dv, \quad \rho u = \int_0^{v_{\max}} v f\, dv. \tag{2.4}$$

Testing with other functions $\phi(v) = v^\gamma$ for $\gamma = 1, 2 \ldots$, one can obtain a coupled hierarchy of models. We are interested in the first-moment approximation (2.3). However, Eq. (2.3) is a partial differential equation in $\rho$ and $u$. Unless one assumes an explicit dependence between $\rho$ and $u$, it cannot be solved. This is known to be the closure problem. There exist

many possible closure relations for system (2.2). As in [21], here, also we consider stationary solutions of the space homogeneous kinetic equation., i.e., $f^e$ such that $C(f^e) = 0$ to close the system. It can be shown [21] that there exists a one-parameter family of solutions to $C(f^e) = 0$ depending on the density $\rho$: For any fixed density $\rho$ we have that $f^e(\rho, v)$ is a solution. Therefore, we close the LWR–model by the equilibrium velocity defined as

$$u^e(\rho) = \frac{1}{\rho} \int_0^{v_{\max}} v f^e(\rho, v) dv. \tag{2.5}$$

The precise form of $f^e$ is given in Section 5 of [21]. For the following discussion it is only necessary to observe that the function $u^e(\rho)$ is a monotone nonincreasing function in $\rho$. We give a plot of the flux function

$$g(\rho) = \rho u^e(\rho) \tag{2.6}$$

in Fig. 4.1 and it can be approximated by a triangular-shaped fundamental diagram. However, the following discussion holds true in more general cases, namely for flux functions being smooth, concave and having a single maximum.

## 3. The macro-kinetic hybrid model

Before introducing our hybrid model, let us present some basic notations and definitions to be used in the sequel.

**Definition 3.1.** A road network is a finite connected directed graph consisting of $\mathcal{K}$ arcs and $\mathcal{N}$ vertices. The arcs and the vertices correspond to roads and junctions, respectively.

For a given junction $n$ we denote by $\delta_n^+$ the set of indices of all the incoming roads to $n$ and by $\delta_n^-$ the set of indices of all the outgoing roads to $n$.

Each road $i$ is modeled by an interval $I_i = [a_i, b_i]$, possibly with either $a_i = -\infty$ or $b_i = +\infty$. At a given junction $n$, we denote the junction point by $x_0 = a_i$ if $i \in \delta_n^+$ and $x_0 = b_i$ if $i \in \delta_n^-$.

We want to use the kinetic description to derive coupling conditions at the junction. These conditions are used in the macroscopic model as explained below. In this way we obtain a hybrid model allowing on the one hand the precise description near the junction and a coarse (but computationally inexpensive) LWR-model on the road. The more detailed view on the dynamics at the junction is motivated by the fact that one needs a more detailed model to describe the dynamics properly. The kinetic equation allows, for example, to distribute cars by their velocity, which is, e.g., the case at highway off-ramps.

We proceed as follows: first, we derive the necessary coupling conditions for the kinetic model. Second, these conditions are used later to compute the mass fluxes through a junction. And finally, the mass fluxes are then used as boundary conditions for the macroscopic model.

At a junction, we consider the Boltzmann type model (2.1) on each road $i \in \delta^+ \cup \delta^-$

$$\partial_t f_i + v \partial_x f_i = C(f_i), \quad x \in [a_i, b_i], \quad t > 0, \quad v \in [0, v_{\max}]. \tag{3.1}$$

On each road $i$ of the network, we are interested in weak solutions to (3.1), i.e., such that

$$\sum_{i \in \mathcal{K}} \left( \int_0^{v_{\max}} \int_0^{+\infty} \int_{a_i}^{b_i} (f_i \partial_t \varphi_i + v f_i \partial_x \varphi_i - C(f_i)\varphi_i) \, dx \, dt \, dv \right) = 0 \tag{3.2}$$

holds for any set of smooth functions $\{\varphi_i\}_{i\in\mathcal{K}} : I_i \times [0,+\infty[\times[0,v_{\max}] \longrightarrow \mathbb{R}$ with compact support. Furthermore, here we assume that $\varphi$ is also smooth across a junction, i.e.,

$$\varphi(b_i) = \varphi(a_j), \quad \forall i \in \delta^- \ \text{ and } \ \forall j \in \delta^+. \tag{3.3}$$

The braking and acceleration force is neglected at the junction, since a junction represents a single point in space only. Furthermore, we obtain from (3.2) for each single junction $n$

$$\sum_{j\in\delta_n^+} v f_j(x_0,v,t) = \sum_{j\in\delta_n^-} v f_j(x_0,v,t) \tag{3.4}$$

by using compactly supported test functions with property (3.3) and sufficiently regular functions $f_j$. Since $v \geqslant 0$, we can only prescribe boundary conditions for (3.1) at $x = a_i$. Nevertheless, relation (3.4) does not uniquely define the boundary conditions for the outgoing roads. In order to remedy this fact, like in the modeling of macroscopic traffic flow, we propose the following:
For a given junction, let us denote by $\alpha_{i,j}^v$ the percentage of cars with velocity $v$ on road $i$, going to road $j$. The corresponding matrix $A := (\alpha_{i,j}^v)_{i\in\delta^-,j\in\delta^+,\forall v\in[0,v_{\max}]}$ is assumed to be known a priori (see [4, 6, 17]). By definition, we have

$$\forall v \in [0,v_{\max}], \quad \sum_{j\in\delta^+} \alpha_{i,j}^v = 1 \quad \forall\ i \in \delta^-. \tag{3.5}$$

Therefore, for any given junction, the boundary conditions for $\{f_l\}_{l\in\delta_n^\pm}$ are

$$v f_j(x_0^-,t,v) = \sum_{i\in\delta^-} \alpha_{i,j}^v v f_i(x_0^+,t,v), \ \ \forall\ v \in [0,v_{\max}]. \tag{3.6}$$

Clearly, condition (3.6) implies (3.4). In contrast to macroscopic modeling the percentages $\alpha_{i,j}^v$ are additionally velocity dependent. This is the case, e.g., at a highway off-ramp, where only cars which are slowing down exit but faster ones stay. Condition (3.6) is sufficient to determine the necessary boundary conditions for (3.1). However, we use (3.6) to obtain conditions for the first moment approximation to (3.1), namely, the LWR-model. This constitutes the hybrid character of the model. According to (2.4), the following quantities can be computed from a solution to the kinetic model:

$$\rho_l = \int_0^{v_{\max}} f_l(x_0,t,v)\,dv, \quad q_l = \int_0^{v_{\max}} v f_l(x_0,t,v)\,dv. \tag{3.7}$$

Before proceeding with the derivation of macroscopic coupling conditions, we briefly discuss some properties of the LWR model (2.3) for a flux function (2.6) having the properties of being concave with a single maximum. As in [22], we introduce the demand and supply functions for a general flux function $g(\rho)$. The demand and supply functions are defined as the increasing and decreasing parts of the curve $\rho \longmapsto \rho u(\rho) = g(\rho)$, respectively, as depicted in Figs. 3.1 and 3.2. The demand at a given point is interpreted as the amount of flux that can be sent from this point, while the supply is the quantity of flux that can be received at this point.

The demand and supply functions have a relation with Riemann problems for (2.3). A Riemann problem is the following initial-value problem:

$$\partial\rho + \partial_x g(\rho) = 0, \quad \rho_0(x) = \begin{cases} \rho_l, & x < 0 \\ \rho_r, & x > 0, \end{cases} \tag{3.8}$$

A solution to the Riemann problem (3.8) consists of either a shock wave (corresponding to a braking) or a rarefaction wave (corresponding to an acceleration), depending on values of $\rho_l$ and $\rho_r$. Indeed,

$(i)$ if $\rho_l \leqslant \rho_r$, the solution consists of a shock wave connecting $\rho_l$ to $\rho_r$, viz.

$$\rho(x,t) = \begin{cases} \rho_l, & \text{if } \ x < (g(\rho_r) - g(\rho_l))/(\rho_r - \rho_l), \quad t \geqslant 0, \\ \rho_r, & \text{if } \ x > (g(\rho_r) - g(\rho_l))/(\rho_r - \rho_l), \quad t \geqslant 0; \end{cases} \tag{3.9}$$

$(ii)$ if $\rho_l > \rho_r$, the solution is a rarefaction wave connecting $\rho_l$ to $\rho_r$, i.e.,

$$\rho(x,t) = \begin{cases} \rho_l, & \text{if } \ x \leqslant g'(\rho_l)t, \quad t \geqslant 0, \\ (g')^{-1}(x/t), & \text{if } \ g'(\rho_l) \leqslant x \leqslant g'(\rho_r), \quad t \geqslant 0, \\ \rho_r, & \text{if } \ x > g'(\rho_r)t, \quad t \geqslant 0. \end{cases} \tag{3.10}$$

Now, for a given data $\rho_l$, we can compute the demand $d(\rho_l)$. For any flux $0 \leqslant q \leqslant d(\rho_l)$, we can solve the Riemann problem and obtain shock or rarefaction waves having nonpositive speed. Conversely, if $0 \leqslant q \leqslant s(\rho_r)$ we obtain only waves of nonnegative speed. Considering now the situation at a junction, we can only prescribe on *incoming* roads mass fluxes less than the actual demand $d(\rho_i(a_i,t))$. On *outgoing* roads we can only prescribe mass fluxes less than the actual supply $s(\rho_i(b_i,t))$.

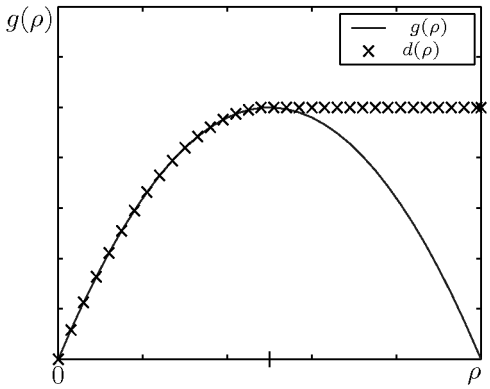


Fig. 3.1. The demand function

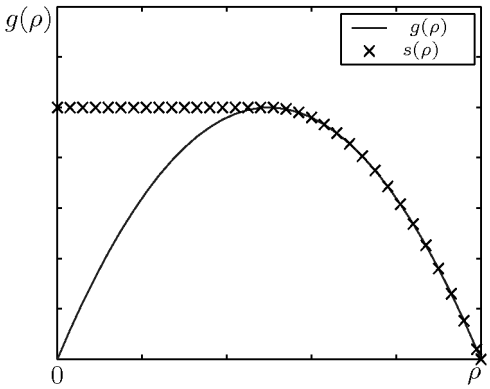


Fig. 3.2. The supply function

Next, we combine the previous discussions to find solutions to the following macroscopic problem: We consider weak solutions to the macroscopic model (2.3) on each road $i \in \delta^+ \cup \delta^-$

$$\partial_t \rho_i + \partial_x g(\rho_i) = 0, \quad x \in [a_i, b_i], \quad t > 0, \tag{3.11}$$

where $g(\rho) := \rho u^e(\rho)$ and initial data

$$\rho_i(x,0) = \rho_{i,0}(x), \quad x \in [a_i, b_i]. \tag{3.12}$$

Weak solutions to (3.11), (3.12) satisfy

$$\sum_{i \in \mathcal{K}} \left( \int_0^{+\infty} \int_{a_i}^{b_i} (\rho_i \partial_t \varphi_i + g(\rho_i) \partial_x \varphi_i) \, dx \, dt + \int_{a_i}^{b_i} \rho_{i,0} \varphi(x,0) \, dx \right) = 0. \tag{3.13}$$

At a given junction we obtain

$$\sum_{j\in\delta^+} g(\rho_j(x_0,t)) = \sum_{j\in\delta^-} g(\rho_j)(x_0,t). \tag{3.14}$$

In order to fulfill this condition we use the kinetic conditions derived before. This amounts to solve the following hybrid problem at the junction, in which we maximize the total mass flux passing through the junction i.e., the flux is given by the solution to the problem.

$$\max \sum_{j\in\delta^+} \int_0^{v_{\max}} v f_j(x_0^+,t,v)\,dv \quad \text{subject to} \quad \int_0^{v_{\max}} f_i(x_0^-,t,v)\,dv = \rho_i(x_0^-,t), \quad \forall i\in\delta^-;$$

$$v f_j(x_0^-,t,v) = \sum_{j\in\delta^+} \alpha_{i,j}^v v f_i(x_0^+,t,v), \quad \forall v\in[0,v_{\max}];$$

$$\int_0^{v_{\max}} v f_i(x_0^-,t,v)dv \leqslant d_i, \quad \forall i\in\delta^-; \quad \int_0^{v_{\max}} v f_j(x_0^+,t,v)dv \leqslant s_j, \quad \forall j\in\delta^+;$$

$$f_j(x_0^-,t,v) \geqslant 0, \quad \forall j\in\delta^+; \quad f_i(x_0^-,t,v) \geqslant 0, \quad \forall i\in\delta^-. \tag{3.15}$$

Some remarks are in order. The solution clearly satisfies (3.4) and therefore

$$\sum_{i\in\delta^-} \int_0^{v_{\max}} v f_i(x_0^-,t,v)\,dv = \sum_{j\in\delta^+} \int_0^{v_{\max}} v f_j(x_0^+,t,v)\,dv \tag{3.16}$$

and hence also (3.14). Next, we show that for piecewise constant initial data and an arbitrary discretization in the variable $v$, the problem at the junction has a solution. The mass flux through a junction depends on the boundary conditions on either side of the junction and due to the previous discussion has therefore to satisfy

$$\int_0^{v_{\max}} v f_i(x_0^-,t,v)dv \leqslant d_i, \quad \forall i\in\delta^-, \quad \int_0^{v_{\max}} v f_j(x_0^+,t,v)dv \leqslant s_j, \quad \forall j\in\delta^+,$$

where $d_i := d(\rho_i^-)$ and $s_j := s(\rho_j^+)$ are the demand on the incoming road $i$ and the supply on the outgoing road $j$, respectively.

**Construction of the Riemann solution at a junction.** We construct a solution to the maximization problem using piecewise constant data and a discretization in the $v$-space. This is later used in the numerical simulations to obtain the conditions at the junction as well as the numerical boundary conditions. Let us consider a discrete version of the problem (3.15) i.e. $v\in\{v_1,v_2,\dots v_N\}$ with $N\in\mathbb{N}$. We pose

$$f_i(x_0^-,t,v_k) = f_{i,k}, \quad i\in\delta^-, \quad k=1,\dots,N,$$

$$f_j(x_0^+,t,v_k) = f_{j,k}, \quad j\in\delta^+ \quad k=1,\dots,N.$$

Therefore, the problem (3.15) becomes a linear program with unknowns $\{f_{l,k}\}_{l\in\delta^+\cup\delta^-,k=1,\dots,N}$.

**Proposition 3.1.** *Let $U_i^- = (\rho_i^-, q_i^- = \rho_i^- u(\rho_i^-))$, $i \in \delta^-$, and $U_j^+ = (\rho_j^+, q_j^+ = \rho_j^+ u(\rho_j^+))$, $j \in \delta^+$, some initial macroscopic boundary data respectively on incoming and outgoing roads of a junction. Then there exist some unique intermediate states $U_i^+ = (\rho_i^+, q_i^+)$, $i \in \delta^-$, and $U_j^- = (\rho_j^-, q_j^-)$, $j \in \delta^+$, solution to the Riemann problem at the junction and such that the mass fluxes*

$$q_i^+ = \sum_{k=1}^{N} v_k f_{i,k}, \quad i \in \delta^-, \quad \text{and} \quad q_j^- = \sum_{k=1}^{N} v_k f_{j,k}, \quad j \in \delta^+,$$

*are given by a solution of a discrete version of* (3.15).

*Proof.* First of all we neglect the case of stationary shocks: if $q_i^+ = d(\rho_i^-)$ we set $U_i^+ := U_i^-$ and if $q_j^- = s(\rho_j^+)$ we set $U_j^- := U_j^+$. As the problem (3.15) has no contradictory constraints, therefore it admits a solution for any macroscopic boundary data $U_i^-$ and $U_j^+$. Thus, there exist some mass fluxes

$$0 \leqslant q_i^+ = \sum_{k=1}^{N} v_k f_{i,k} \leqslant d_i \ \forall\, i \in \delta^- \ \text{ and}$$

$$0 \leqslant q_j^+ = \sum_{k=1}^{N} v_k f_{j,k} \leqslant s_j, \ \forall\, j \in \delta^+$$

which correspond to the flux values at the unknown intermediate states $U_i^+$ and $U_i^-$, respectively.

Having the values of $q_i^+$ and $q_j^-$ at hand, the right intermediate state $U_i^+$ (resp. $U_j^-$) on the fundamental diagram is the one that can be connected to $U_i^-$ (resp. $U_j^+$) with a shock wave (see Eq. (3.9)) or a rarefaction wave (see Eq. (3.10)) with nonpositive speed (resp. nonnegative speed). □

## 4. Numerical applications and comparison with the fully macroscopic model

In this section we are interested in traffic dynamics for the setup depicted in Fig. 4.2. We consider a ring road with an off-ramp and an on-ramp located at $x = 0 = 100$ and $x = 50$, respectively. To provide a deeper insight into the above hybrid formulation, we consider for the kinetic model a discrete velocity distribution, i.e., $v \in \{v_1, \dots v_N\}_{N \in \mathbb{N}}$. For the macroscopic part, we use the following form of $u^e$:

$$u^e(\rho) = \begin{cases} \dfrac{q^*}{\rho^*}, & 0 \leqslant \rho \leqslant \rho^*, \\ \dfrac{1}{\rho}\left(q^* - \dfrac{q^*}{\rho_{\max} - \rho^*}(\rho - \rho^*)\right), & \rho^* \leqslant \rho \leqslant \rho_{\max} = 1, \end{cases} \tag{4.1}$$

where $q^*$ is the maximal flux and $\rho^*$ is the corresponding density.

This yields to a triangular fundamental diagram (see the solid curve in Fig. 4.1). In the examples below, we consider different traffic situations on the ring road in Fig. 4.2 and compare numerical simulations given by the hybrid model with those obtained with the fully macroscopic model.

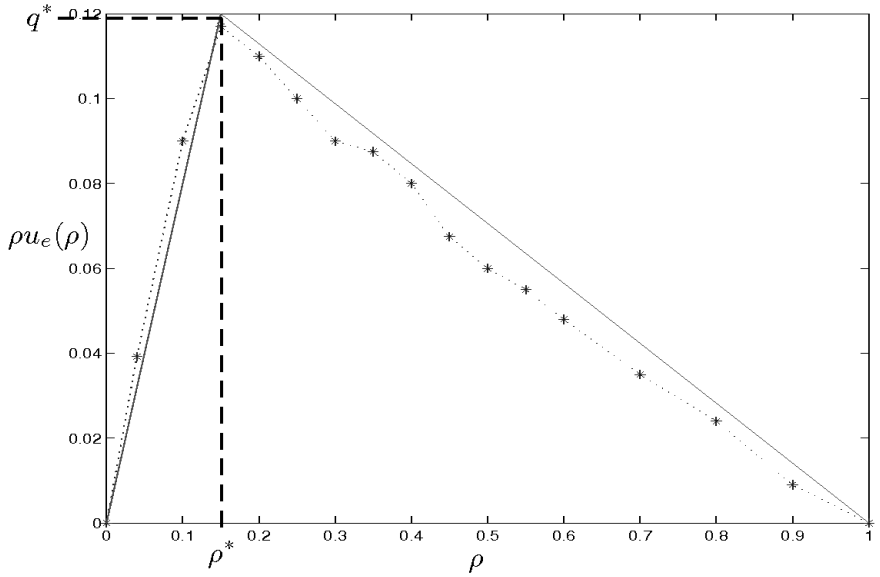


Fig. 4.1. Solid line — the fundamental diagram considered here. Doted curve — the fundamental diagram considered in [21]

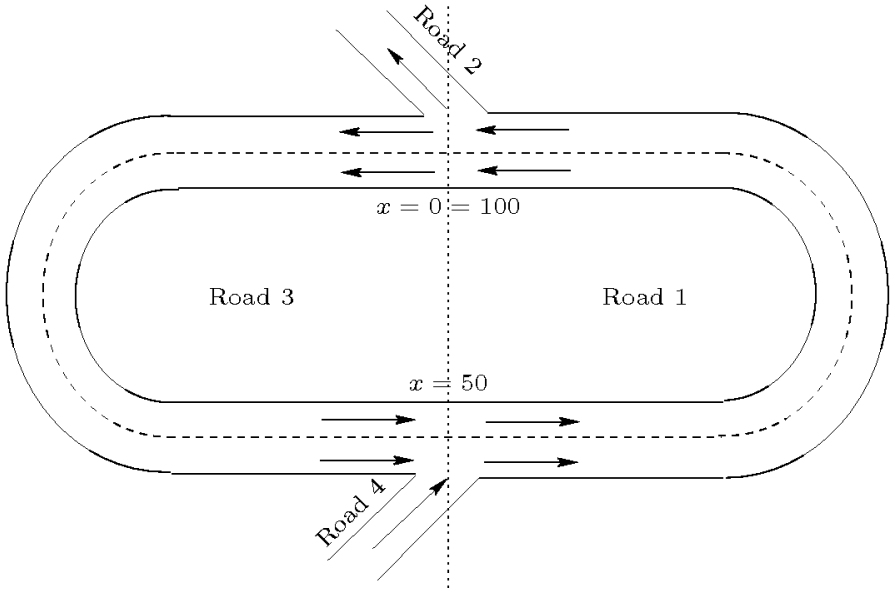


Fig. 4.2. A ring road with an off-ramp and an on-ramp located respectively at $x = 0 = 100$ and at $x = 50$

**Example 4.1 (on-ramp).** In this example we consider the case $N = 4$, i.e., $v \in \{v_1, v_2, v_3, v_4\}$. We start the simulation with Road 1 and Road 3 empty. We set the percentage of cars aiming to enter on Road 2 to zero and we keep a nonzero constant demand on Road 4 during the simulation time in order to observe the impact of the velocity distribution at an on-ramp. In Fig. 4.3, we present some numerical results of the hybrid model with constant velocity distribution (i.e., $v_1 = v_2 = v_3 = v_4$) and those obtained with the fully macrosocpic model, for the same initial and boundary conditions. For the fully macroscopic model the mass flux through the junction depends only on the priority rule (which depends on the demands on incoming roads), whereas the kinetic approach considers the velocity distribution without any priority rule. The consequence of the velocity distribution can be observed in Fig. 4.4 where we present some numerical simulations of the hybrid model with varying velocity distributions.

**Example 4.2 (dependence on the numbers of velocities).** Here we consider the hybrid model with different values of $N$. And as in Example 4.1, we start the simulation with Road 1 and Road 3 empty. We set the percentage of cars aiming to enter on Road 2 to zero and we keep a nonzero constant demand on Road 4 during the simulation time in order to observe the impact of the value of $N$ on traffic dynamics at an on-ramp. Figure 4.5 presents the numerical results of the hybrid model with a uniform velocity distribution varying the parameter $N$ and those obtained with the fully macrosocpic model, for the same initial and boundary conditions.

**Example 4.3 (velocity dependent distributions).** We consider again the case $N = 4$, i.e., $v \in \{v_1, v_2, v_3, v_4\}$. We start the simulation with Road 1 and Road 3 empty. In contrast with the previous examples, here the percentage of cars aiming to enter on Road 2 is computed according to the velocity of vehicles. More precisely, we consider an exit to a highway with the following conditions:

$$\alpha_{1,2}^k = \begin{cases} 1 & \text{if} \quad v_k \leqslant v_{\max}/2, \\ & \qquad\qquad \forall\, k = 1, \ldots, N. \\ 0 & \text{if} \quad v_k > v_{\max}/2, \end{cases} \tag{4.2}$$

We keep a nonzero constant demand on Road 4 and a nonzero constant supply on Road 2 during the simulation time. Figure 4.6 presents some numerical simulations obtained with the hybrid model and the fully macrosocpic model for the same initial and boundary conditions. For the fully macroscopic model, the percentage of vehicles aiming to enter on Road 2 is obtained from (4.2) in the following way:

$$\alpha_{1,2} = \frac{\sum_{k=1}^N \alpha_{1,2}^k}{\sum_{k=1}^N \alpha_{1,2}^k + \sum_{k=1}^N \alpha_{1,3}^k}. \tag{4.3}$$

**Example 4.4 (time-dependent inflow).** In this section we consider a more general situation which consists of a nonconstant demand on Road 4 and some time-dependent parameters $\alpha_{1,2}^k$. We consider again the case $N = 4$, i.e., $v \in \{v_1, v_2, v_3, v_4\}$ and we start the simulation with Road 1 and Road 3 empty. We present some numerical results given by the hybrid model with different settings of $\alpha_{1,2}^k(t)$ in Fig. 4.7.

## 5. Concluding remarks

We propose a new hybrid model for an heterogeneous flow on road networks. The distinctive feature of this model is that it includes the velocity distribution in the flow, which has some consequences on the traffic dynamics, in particular, at intersections. Furthermore, this model does not require any additional conditions expressing how the available space on the outgoing road is shared by the flows on the incoming roads. This hybrid model based on the coupling of the LWR macroscopic model and a kinetic type model offers an appropriate trade-off between accuracy and computational complexity, therefore suitable for on-line prediction. Future research topics may include the calibration of the model parameters based on measured traffic data and the refinement of the model too.

**Acknowledgements.** This work was supported by the Kaiserslautern Excellence Cluster "Dependable Adaptive Systems and Mathematical Modelling" and DAAD grant D/06/19582 and DFG grant HE5386/6–1.

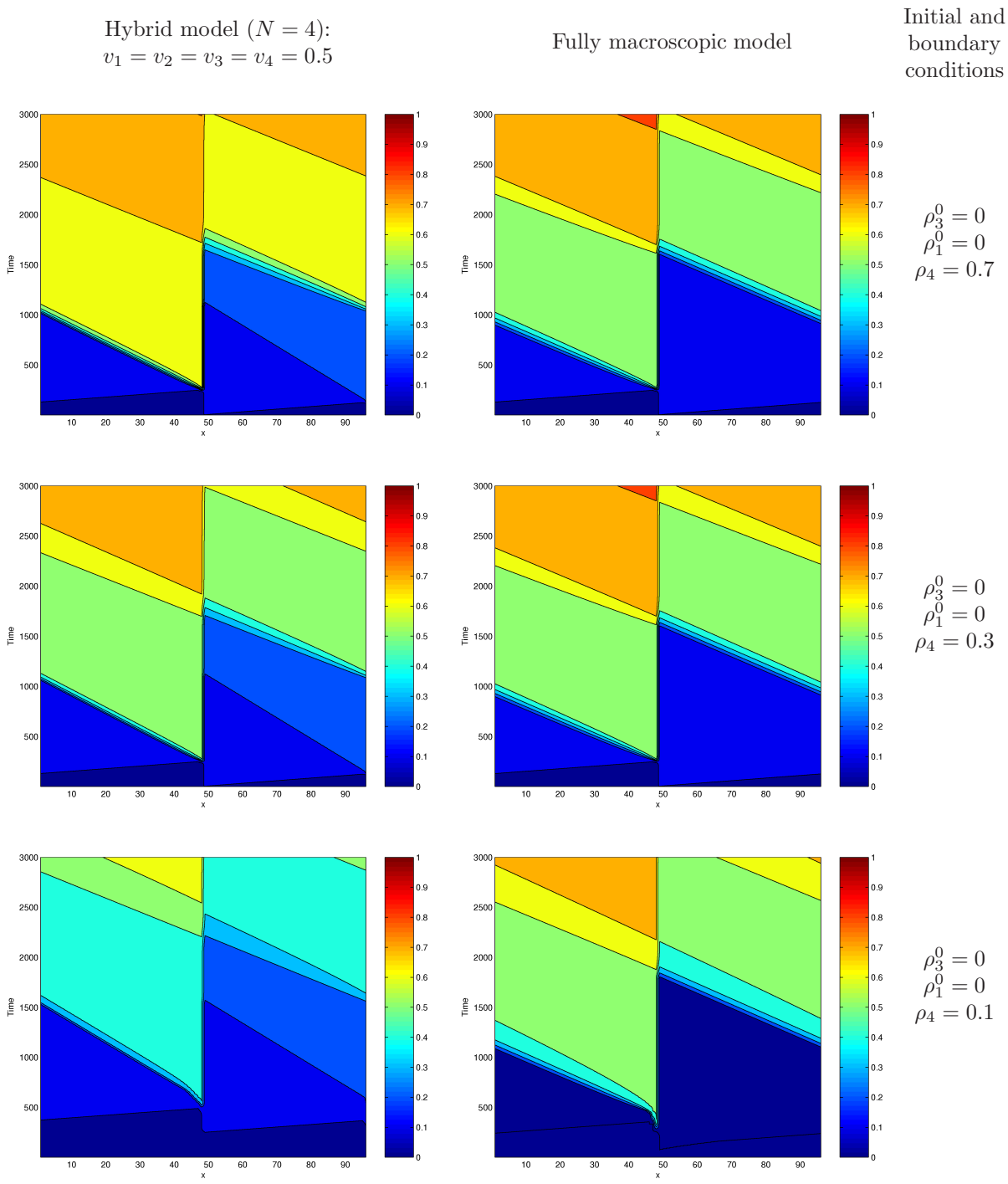


F i g. 4.3. Traffic dynamics on a highway bottleneck caused by an on-ramp. The plots show the traffic dynamics on Road 3 (corresponding to the section between $x = 0$ and $x = 50$) and Road 1 (corresponding to the section between $x = 50$ and $x = 100$) when the percentage of vehicles aiming to enter on Road 2 is equal to zero. The column on the left shows the evolution of the density of vehicles given by the macro-kinetic hybrid model with constant velocity distribution $\{v_1 = v_2 = v_3 = v_4 = 0.5\}$, whereas the column on the right shows the corresponding result given by the fully macroscopic model. The rows correspond to different simulation runs varying the boundary condition on Road 4

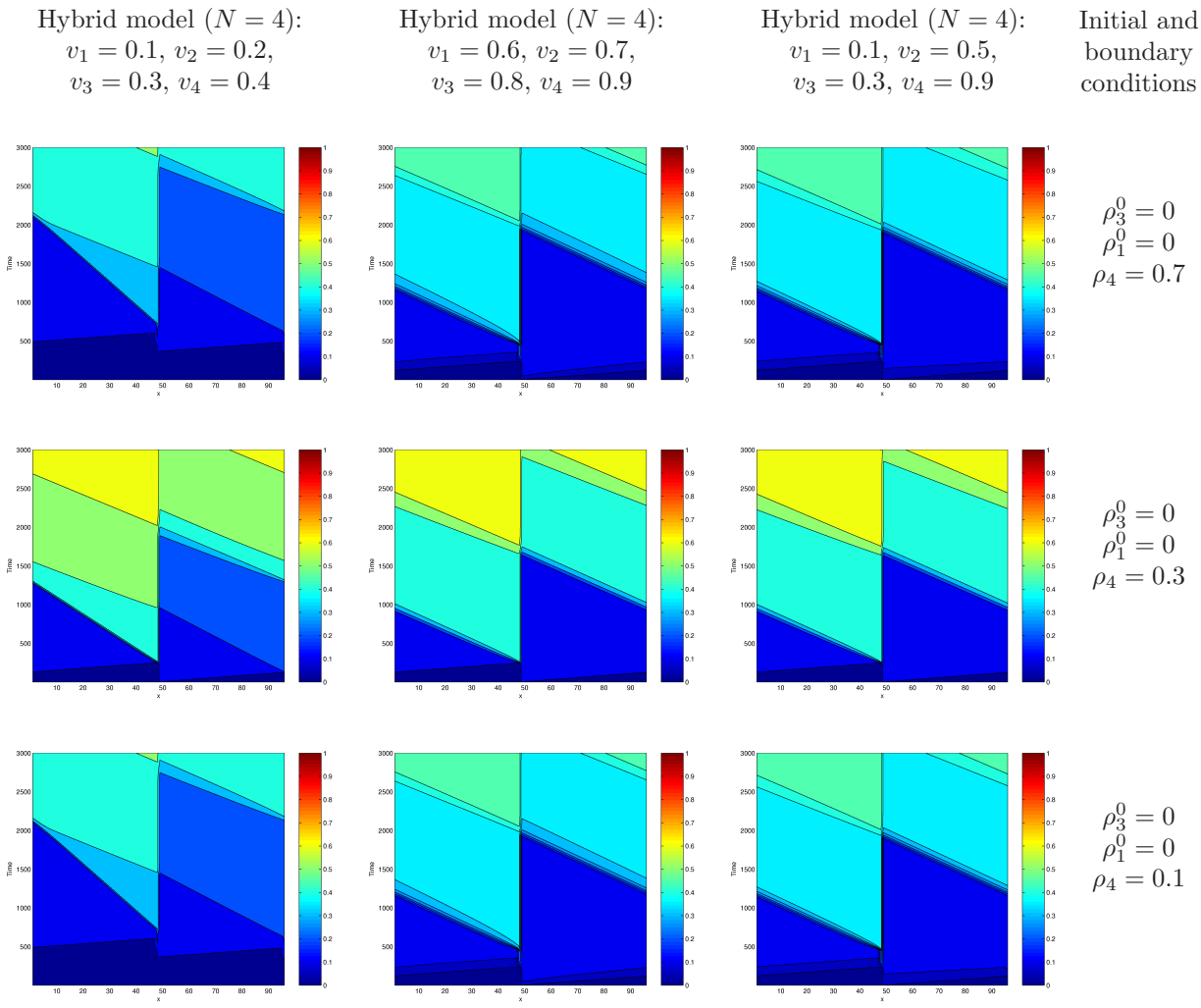


Fig. 4.4. Traffic dynamics on a highway bottleneck caused by an on-ramp. The plots show the traffic dynamics on Road 3 (corresponding to the section between $x = 0$ and $x = 50$) and Road 1 (corresponding to the section between $x = 50$ and $x = 100$) obtained with the macro-kinetic hybrid model when the percentage of vehicles aiming to enter on Road 2 is equal to zero. The columns on the left, in the center and on the right show the evolution of the density with the velocity distributions $\{v_1 = 0.1, v_2 = 0.2, v_3 = 0.3, v_4 = 0.4\}$, $\{v_1 = 0.6, v_2 = 0.7, v_3 = 0.8, v_4 = 0.9\}$, $\{v_1 = 0.1, v_2 = 0.5, v_3 = 0.3, v_4 = 0.9\}$, respectively. The rows correspond to different simulation runs varying the boundary condition on Road 4

Hybrid model ($N = 2$):
$v_1 = 1/3$, $v_2 = 2/3$

Hybrid model ($N = 4$):
$v_1 = 1/5$, $v_2 = 2/5$,
$v_3 = 3/5$, $v_4 = 4/5$

Initial and boundary conditions

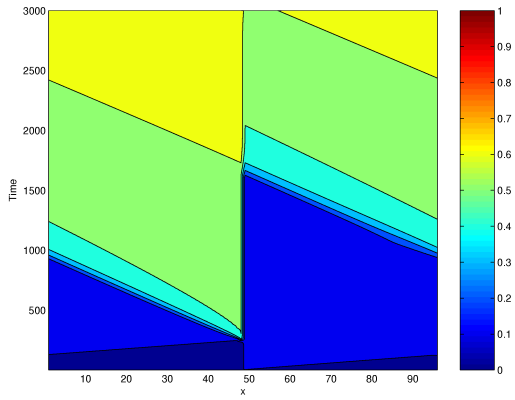


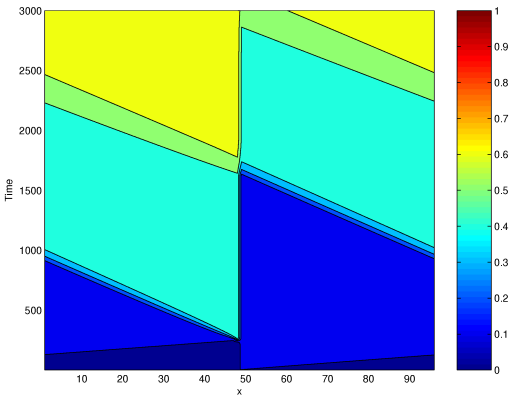


$\rho_1^0 = 0$
$\rho_3^0 = 0$
$\rho_4 = 0.3$

Hybrid model ($N = 8$):
$v_1 = 1/9$, $v_2 = 2/9$, $v_3 = 3/9$,
$v_4 = 4/9$, $v_5 = 5/9$, $v_6 = 6/9$,
$v_7 = 7/9$, $v_8 = 8/9$

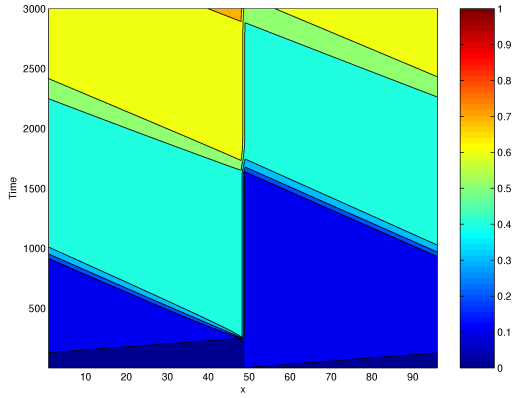


Fully macroscopic model

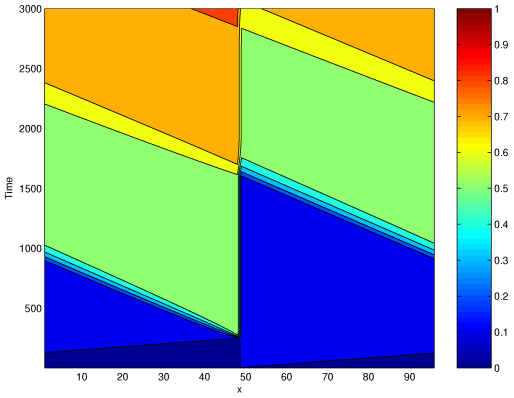


$\rho_1^0 = 0$
$\rho_3^0 = 0$
$\rho_4 = 0.3$

F i g. 4.5. Traffic dynamics on a highway bottleneck caused by an on-ramp. The plots show the traffic dynamics on Road 3 (corresponding to the section between $x = 0$ and $x = 50$) and Road 1 (corresponding to the section between $x = 50$ and $x = 100$) obtained with the macro-kinetic hybrid model varying the parameter $N$ (related to the velocity distribution) and the fully macroscopic model, respectively

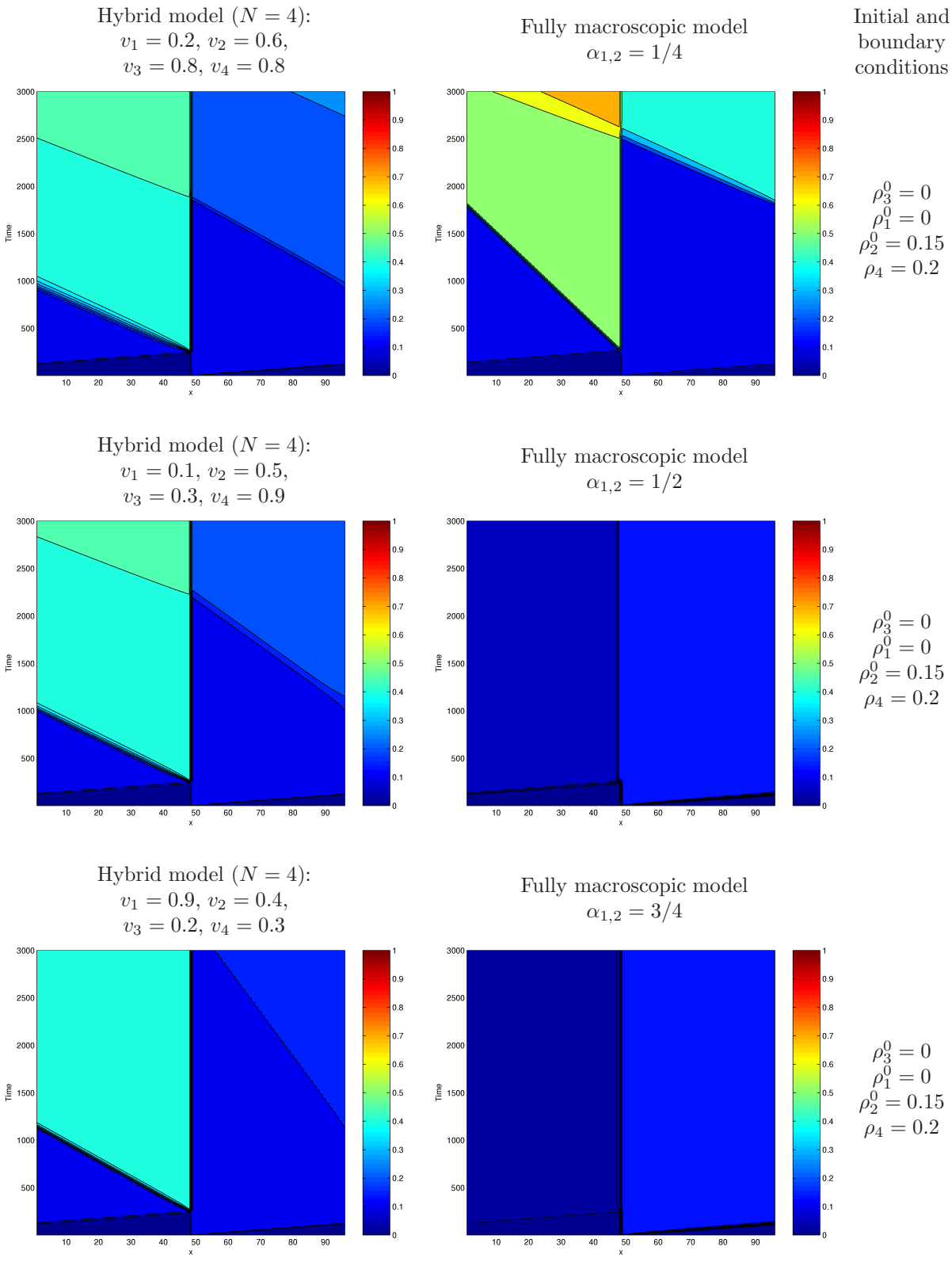


Fig. 4.6. Traffic dynamics on a highway bottleneck caused by an on-ramp and an off-ramp. The plots show the traffic dynamics on Road 3 (corresponding to the section between $x = 0$ and $x = 50$) and Road 1 (corresponding to the section between $x = 50$ and $x = 100$) when the percentage of cars aiming to enter on Road 2 depends on the velocity. The column on the left shows the evolution of the density given by the macro-kinetic hybrid model with the velocity distributions $\{v_1 = 0.2, v_2 = 0.6, v_3 = 0.7, v_4 = 0.8\}$, $\{v_1 = 0.1, v_2 = 0.5, v_3 = 0.3, v_4 = 0.9\}$, $\{v_1 = 0.9, v_2 = 0.4, v_3 = 0.2, v_4 = 0.3\}$ from top to bottom respectively, and the column on right shows the corresponding results obtained with the fully macroscopic model

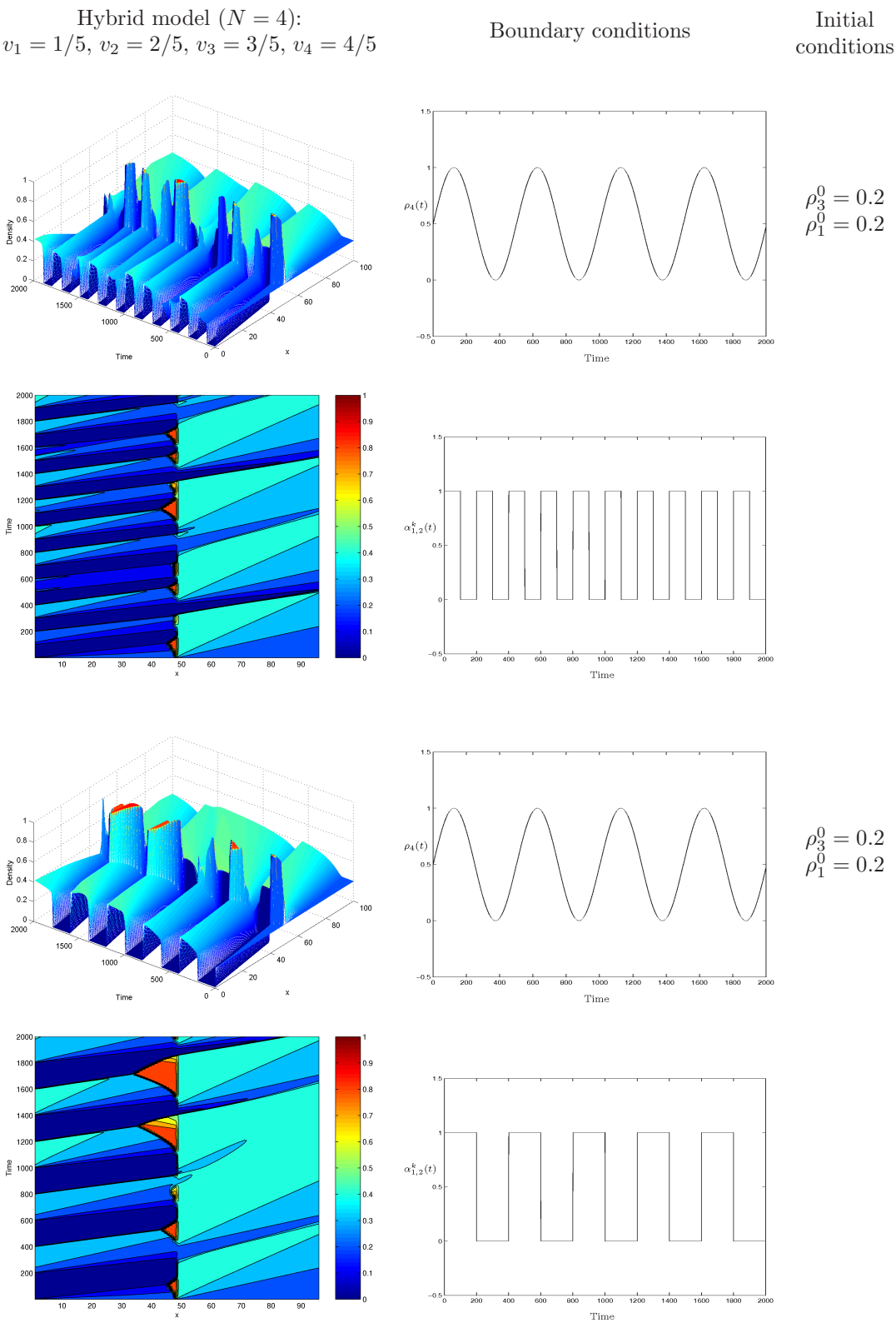


F i g. 4.7. Traffic dynamics on a highway bottleneck caused by an on-ramp and an off-ramp. The plots show the traffic dynamics on Road 3 (corresponding to the section between $x = 0$ and $x = 50$) and Road 1 (corresponding to the section between $x = 50$ and $x = 100$) obtained with the macro-kinetic hybrid model when the demand on Road 4 and the percentage of cars aiming to enter on Road 2 are time dependent. The column on the left shows the evolution of the density with the velocity distributions $\{v_1 = 1/5, v_2 = 2/5, v_3 = 3/5, v_4 = 4/5\}$ and the column on the right shows the boundary conditions on Road 4 and the distribution parameter $\alpha^k_{1,2}$, $k = 1 \dots 4$

## References


1. B. Argall, E. Cheleshkin, J. M. Greenberg, C. Hinde, and P. J. Lin, *A rigorous treatment of a follow-the-leader traffic model with traffic lights present*, SIAM J. Appl. Math., **63** (2002), pp. 149–168.

2. A. Aw and M. Rascle, *Resurrection of "second order" models of traffic flow?*, SIAM J. Appl. Math., **60** (2000), pp. 916–938.

3. R. E. Chandler, R. Herman, and E. Montroll, *Traffic dynamics: Studies in car following*, Oper. Res., **6** (1958), pp. 165–184.

4. G. M. Coclite, M. Garavello, and B. Piccoli, *Traffic flow on a road network*, SIAM J. Math. Anal., **36** (2005), pp. 1862–1886.

5. C. M. Dafermos, *Hyperbolic Conservation Laws in Continuum Physics*, Springer Verlag, 2000.

6. M. Garavello and B. Piccoli, *Source-Destination flow on a road network*, Commun. Math. Sci., **3** (2005), pp. 261–283.

7. J. Greenberg, *Extension and amplification of the Aw-Rascle model*, SIAM J. Appl. Math., **63** (2001), pp. 729–744.

8. B. Haut and G. Bastin, *A second order model of road junctions in fluid models of traffic networks*, Netw. Heterog. Media, **2** (2007), pp. 227–253.

9. D. Helbing, A. Hennecke, V. Shvetsov, and M. Treiber, *Micro and macro simulation of freeway traffic*, Math. Comp. Model., **35** (2002), pp. 517–547.

10. R. Herman and I. Prigogine, *Kinetic Theory of Vehicular Traffic*, American Elsevier, New York, 1971.

11. M. Herty and R. Illner, *On Stop-and-Go Waves in Dense Traffic*, Kine. Relat. Models, **1** (2008), pp. 437–452.

12. M. Herty, R. Illner, A. Klar, and V. Panferov, *Qualitative properties of solutions to systems of Fokker-Planck equations for multilane traffic flow* Transp. Theory Stat. Phys., **35** (2006), pp. 31–54.

13. M. Herty, C. Kirchner, and S. Moutari, *Multi-Class Traffic Models For Road Networks*, Commun. Math. Sci., **4** (2006), pp. 591–608.

14. M. Herty, C. Kirchner, S. Moutari, and M. Rascle, *Multicommodity Flows on Road Nectworks*, Commun. Math. Sci., **6** (2008), pp. 171–187.

15. M. Herty and A. Klar, *Modelling, Simulation and Optimization of Traffic Flow Networks*, SIAM J. Sci. Comp., **25** (2003), pp. 1066–1087.

16. M. Herty, S. Moutari, and M. Rascle, *Optimization criteria for modelling intersections of vehicular traffic flow*, Netw. Heterog. Media, **1** (2006), pp. 275–294.

17. M. Herty and M. Rascle, *Coupling conditions for a class of second order models for traffic flow*, SIAM J. Math. Anal., **38** (2006), pp. 595–616.

18. H. Holden and N. H. Risebro, *A mathematical model of traffic flow on a network of unidirectional roads*, SIAM J. Math. Anal., **26** (1995), pp. 999–1017.

19. R. Illner, A. Klar and T. Materne, *Vlasov-Fokker-Planck models for multilane traffic flow*, Commun. Math. Sci., **1** (2003), pp. 1–12.

20. A. Klar and R. Wegener, *A hierarchy of models for multilane vehicular traffic I: Modeling*, SIAM J. Appl. Math., **59** (1999), pp. 983–1001.

21. A. Klar and R. Wegener, *Kinetic derivation of macroscopic anticipation models for vehicular traffic*, SIAM J. Appl. Math., **60** (2000), pp. 1749–1766.

22. J. P. Lebacque and M. Khoshyaran, *First order macroscopic traffic flow models: Intersection modeling, Network modeling*, Proceedings of the 16$^{\text{th}}$ International Symposium on Transportation and Traffic Theory (ISTTT), Elsevier (2005) pp. 365–386.

23. M. Lighthill and J. Whitham, *On kinematic waves*, Proc. Roy. Soc. London Ser. A, **229** (1955), pp. 281–345.

24. L. Magne, S. Rabut and J. F. Gabard, *Towards an hybrid macro-micro traffic flow simulation model*, INFORMS Spring Meeting, Salt Lake City, Utah (USA), 2000.

25. S. Moutari and M. Rascle, *A hybrid lagrangian model based on the Aw-Rascle traffic flow model*, SIAM J. Appl. Math., **68** (2007), pp. 413–436.

26. K. Nagel, *Traffic networks*, Handbook on Networks, 2002.

27. P. I. Richards, *Shock waves on the highway*, Oper. Res., **4** (1956), pp. 42–51.

28. F. Siebel and W. Mauser, *Simulating vehicular traffic in a network using dynamic routing*, Math. Comp. Model. Dyn. Syst., **13** (2007), pp. 83–97.

29. J. Smoller, *Shock waves and Reaction-Diffusion Equations*, Springer-Verlag, Heidelberg, 1983.

30. H. M. Zhang, *A non-equilibrium traffic model devoid of gas-like behaviour*, Trans. Res. B, **36** (2002), pp. 275–290.